Carbohydrate Polymers 82 (2010) 920–926

Contents lists available at ScienceDirect

Carbohydrate Polymers

journal homepage: www.elsevier.com/locate/carbpol

Preparation, characterization and biological properties of Gellan gum films with 1-ethyl-3-(3-dimethylaminopropyl)carbodiimide cross-linker

Ming-Wei Lee [a,b,*], Hui-Ju Chen [a], Shu-Wei Tsao [b]

[a] School of Medical Laboratory and Biotechnology, Chung -Shan Medical University, No. 110, Sec. 1, Jianguo N. Rd., Taichung City 402, Taiwan
[b] Department of Clinical Laboratory, Chung Shan Medical University Hospital, No. 110, Sec. 1, Jianguo N. Rd., Taichung City 402, Taiwan

ARTICLE INFO

Article history:
Received 19 April 2010
Received in revised form 24 May 2010
Accepted 10 June 2010
Available online 18 June 2010

Keywords:
Gellan gum
EDC
Biocompatibility
Wound healing

ABSTRACT

Gellan gum (GG) is an exopolysaccharide produced by *Sphingomonas elodea*. To develop a medical application for GG, in this study we prepared 26 μm thick films of GG reacted with 1-ethyl-3-(3-dimethylaminopropyl)carbodiimide (EDC) in 40% ethanol to obtain a cross-linked film (GG40) with 73% gel content and 52.4 MPa tensile strength. *In vitro* biocompatibility tests, GG40 film exhibit nontoxic effects for L929 cells and inhibit absorption and activation of platelets. When implanted into rat subcutaneous tissue, the GG40 film caused minor inflammation in the early postoperative period. The results indicate that the effects of GG40 film on wound healing, wound size reduction (%) and collagen content are higher than those found in commercial products (Duoderm). Therefore, we conclude that the GG film developed in this study has potential for future use in surgical applications.

1. Introduction

Gellan gum (GG) is an exopolysaccharide (EPS), also known as polysaccharide S-60, which is a gelling agent produced by a non-pathogenic strain of *Sphingomonas elodea* ATCC 31461 (Pollock, 1993). Natural GG is a linear electronegative EPS. The main chain of GG consists of four repeating carbohydrates, which includes two D-glucose carbohydrates, one L-rhamnose, and one D-glucuronic acid. In its natural form, GG has two acyl-substituted positions (O-acetate and L-glycerate), which separately connect to the C-6 and C-3 positions of the same glucose molecule. On average, each repeated unit of the main chain has 1 glycerate and 0.5 acetate molecules (Jansson, Lindberg, & Standford, 1983; Jay et al., 1998). GG has the ability to form gel in the presence of cations, but the presence of acetyl groups can interfere with the bonding ability of the ions. The average molecular weight of GG is approximately 500 kDa (Bemiller, 1996).

GG is a food additive approved by the FDA. Although it is extensively used in the foodstuff industry, GG has rarely been investigated for biomedical applications, except for use in drug delivery. Beginning in 2008, Wang, Gong, Lin, Shen, and Wang used modified GG to cultivate human dermalfibroblasts and human fetal osteoblasts. GG has also become an innovative material in applications of tissue engineering. Several advantages of GG are listed here. (1) The GG with heat and acid stability, adjustable elasticity and hardness, and high transmittance (Rinaudo, 2004), which allows the material to easily change form and accommodate many different applications. (2) It has an active reaction group that is suitable for chemical modification, which allows its use in preparing conjugates with molecules of biological activity to increase its range of applications in medical research. (3) GG is a bacterial exopolysaccharide, prepared commercially by aerobic submerged fermentation from *S. elodea*. This process, or the associated purification steps, is not complex (Fialho et al., 2008) and is suitable for development for use in the industry.

The goal of this study is to develop GG for surgical applications by preparing and characterizing a water-insoluble GG film. In addition, this study evaluates the *in vitro* and *in vivo* biocompatibility and effects of cross-linked GG film on wound healing.

2. Methods

2.1. Preparation of GG films

GG of 0.3 g (Sigma G1910) was dissolved in 30 ml de-ionized water (DDW) and heated at 85–90 °C until it became a transparent solution. The solution was then poured onto a glass dish (diameter 10 cm) and evaporated at 37 °C, 1 atm for 3 days to obtain the dry film (GG film). The GG films were then cross-linked by immersing them into an EtOH (ethanol)/DDW solution contain-

* Corresponding author. Tel.: +886 4 24730022x11767; fax: +886 4 23248171.
E-mail address: d880430@csmu.edu.tw (M.-W. Lee).

0144-8617/$ – see front matter © 2010 Elsevier Ltd. All rights reserved.
doi:10.1016/j.carbpol.2010.06.019

ing 15 mM 1-ethyl-3-(3-dimethylaminopropyl)carbodiimide (EDC, sigma 1769), for 24 h at room temperature. To study the effects of the EtOH composition on the EDC cross-linking of the GG, EtOH was diluted in DDW to yield an EtOH/DDW (v/v%) solution. This study used 0%, 20%, 30%, 40%, 50%, 60%, 70%, 80%, 90% and 100% EtOH/DDW. The cross-linked films (denoted as GG0, GG20, GG30, GG40, GG50, GG60, GG70, GG80, GG90 and GG100) were washed with 95% ethanol three times to remove any non-reacted residual EDC and then dried at room temperature (Lee, Hung, Cheng, & Wang, 2005).

2.2. Characterizations of the GG films

An electrical thickness tester (Mitutoyo, MDC-25 SB) was used to measure the thickness of the GG films. We used the FTIR-L396A (Perkin-Elmer) to analyze the properties of the chemical functional groups of the GG films. The analysis of the gel content of the GG films was performed as follows. After drying, we weighed the cross-linked film (W_1) and then swelled it in DDW at 37 °C for 24 h. After removing the wet film from the solution, it was dried in a vacuum oven for 12 h at 60 °C and then weighed again (W_2). The following equation was then used to calculate the gel content of the film (Kenji & Ikada, 1997):

$$\text{Gel content}\,(\%) = \frac{W_2}{W_1} \times 100$$

2.3. Mechanical property measurement

GG films were cut into 1 cm × 5 cm pieces (Kuo et al., 2009). We then used the H1-KS testing machine (Tinius Olsen) with a crosshead speed of 5 mm/min to measure the mechanical properties of the GG films and to automatically record the mechanical parameters.

2.4. Platelet absorption test

Blood drawn from a human body was used to prepare the platelet concentrate. We then prepared and filtered Hepes-Tyrode buffer solution using a 0.45 μm filter. The GG films were then sterilized with 75% ethanol for 24 h. The sterilized films were placed on a 24-well bottom and added with Hepes-Tyrode buffer solution (1 ml) at 37 °C for 15 min. After aspiration of the solution, each well was added with platelet concentrate 1 ml (density $2.9 \times 10^5/\mu l$), and incubated at 37 °C for 120 min. The Automatic Hematology Analyzer (Sysmes KX-21) was then used to determine the number of platelet absorbed on the films. In addition, the SEM (positive control: glass) was used to observe the morphology of the platelets absorbed on the GG films (Ishihara, Nishiuchi, Watanabe, & Iwasaki, 2004).

2.5. MTT assay

The preparation and placement of 11 mm diameter polymeric discs in the bottom of each well of a 48-well tissue-culture plate was used to determine the cell adhesion and the cell growth on the GG films (GG40). We added fibroblast (L-929) cells to the plate with a population of 3×10^4 cells for each well and incubated them at 37 °C. As a positive control, the cells were plated onto 48-well tissue-culture plates (NUNC, Roskilde Denmark). By changing the culture medium, we determined the cell number on each synthetic film after 24, 48, and 72 h of cell seeding by implementing the MTT test. Five independent measurements were conducted for each experimental value (Lee et al., 2005).

2.6. In vivo biocompatibility (subcutaneous implantation)

The purpose of the experiment was to examine the immune compatibilities of GG in an organism. GG40 and Hyaluronic acid (HA) film (control group) were cut into 1.5 cm × 1.5 cm pieces (Ramires, Miccoli, Panzarini, Dini, & Protopapa, 2005). HA as the control group is because it possesses good compatibility (Kenji & Ikada, 1997). The following experimental procedures were then used. SD-rats (male, 250–300 g) were etherized with 4% trichloroacetaldehyde monohydrate (1 mg/ml). We shaved the skin of the animal and disinfected it using iodophor. The polymeric film was implanted in the back of the specimen. The rats were sacrificed on the 3rd, 14th and 30th days after the operation. Five mm wedged tissue were cut from the wound, including the implanted film, granulation tissue, connective tissue, and inferior muscle. The tissues were processed using the standard procedure for histological examinations and their thin sections were examined after staining with Hematoxylin–Eosin (H&E). The animal experiments in this study were approved by the Chung-Shan Medical University Experimental Animal Center.

2.7. Experiment on wound healing

To develop the medical application of GG as a biomedical material, this study was conducted to evaluate the effect of GG on the wound healing process on laboratory rats. Epithelium with an area of 2 cm × 2 cm was cut from the backs of etherized SD-rats (male, 250–300 g). The wound was then treated by applying either commercial Duoderm (control group) or GG40 film (experimental group) and bandaged with gauze. Duoderm is a synthetic dressing, with a bilaminate structure with an outer layer of polyurethane foam and an inner layer that is contain sodium carboxymethylcellulose and gelatin (Leicht, Siim, Dreyer, & Larsen, 1991). Duoderm is the most commonly used dressing in wound care.

Following the sacrifice of the rats after the 5th, 15th, and 24th days, we measured the sizes of the wound area. Reductions in wound size were used as an indicator of wound healing ($n = 4$). The following equation was used to determine the reduction in wound size (Yang, Yang, Lin, Wu, & Chen, 2008):

$$\text{wound size reduction}\,(\%) = \frac{A_0 - A_t}{A_0}$$

where A_0 and A_t are the initial wound area and wound area after time interval 't', respectively. Photographs of the wounds were used for measurement purposes using image analysis software (Image J). Then removed the wound tissue for sectioning (2–3 μm thick) and observed the histology around the wound using H&E staining. In addition, the Masson's trichrome stain was used to observe the formation and distribution of collagen on the wounds (collagen is stained blue). For the relative quantization of collagen, Image J software was used to measure the color values of the blue stain. First, an inverted light microscope (Axiovert 200) was used to record the regenerated tissues using the 20× object lens. The recording position covered all the regenerated tissues. Then, an analysis of the blue color value of each picture was used to determine the average value. A light color and low collagen content indicated a high color value.

2.8. Statistical analysis

Each of the experiments was repeated at least four times, and the values were expressed as means ± standard deviations. For comparison between two groups of data, the Student's t-test was performed. Differences were considered to be statistically significant at $P < 0.05$.

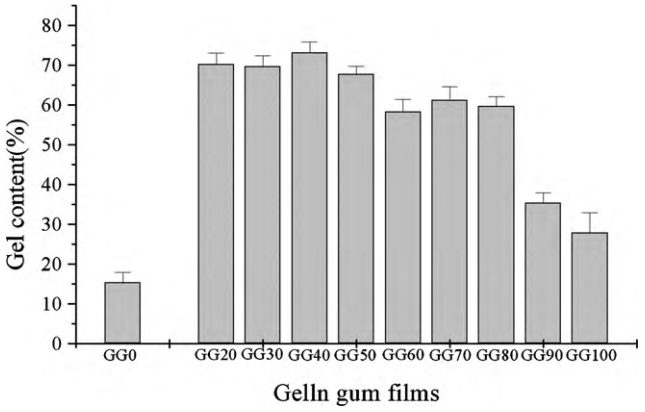

Fig. 1. The gel content of GG films cross-linked in various concentrations of ethanol with 15 mM EDC for 24 h.

3. Results and discussion

3.1. Gel content of cross-linked GG film

EDC is the most widely used reagent for chemical cross-linking. To solve the problem of EDC hydrolysis in water, previous studies (Kwangwoo, Tsuyoshi, Seiichi, & Akio, 2010; Monotalbetti & Falque, 2005) have suggested using a mixture of EtOH/DDW as the reaction solvent. Fig. 1 shows the gel content of GG films cross-linked in various concentrations of ethanol with 15 mM EDC for 24 h. In the control group (without EtOH), the gel content of GG film was found to be only 15 ± 2.0% and showed a poor degree of cross-linking. In 40% ethanol (i.e. GG40 film), the gel content was found to be highest 73 ± 2.6%. In this system the increase of cross-linking degree was not proportional to the ethanol content. This is due to the polymer chain difficulty of the hydrophilic GG to extend in organic solvents, which reduces its reactivity. An ethanol content of 40% was found to be the most suitable condition for cross-linked GG.

3.2. Mechanical properties of GG film

Fig. 2 shows the tensile strength of GG films cross-linked in various concentrations of ethanol with 15 mM EDC for 24 h. The average thickness of films was 26 ± 3 μm. The results indicate that GG30, GG40, and GG50 have high tensile strengths of 45.3 ± 9.6, 52.4 ± 2.3, and 43.2 ± 11.1 MPa, respectively. Previous studies demonstrate that the tensile strength of a polymer is closely correlated to the density of cross-linking (Sen, Majumder, & Bhowmick, 1999; Vijayabaskar, Tikku, B, & Anil, 2006). At lower cross-link density, the tensile strength increases with an increase in the cross-link density. However, at higher cross-link density, the segments of macromolecules become immobile, due to which the system becomes stiff and shows a decrease in elasticity. Based on gel content and mechanical property measurement, GG in 40% ethanol optimizes the cross-linked environment. In summary, with regards to mechanical property, GG40 is suitable for potential application as wound dressing, which has typical values in the range of 2.5–16 MPa (Ezequiel et al., 2009). Therefore, in this study we have selected GG40 as the substrate of choice for evaluating biocompatibility and effects on wound healing.

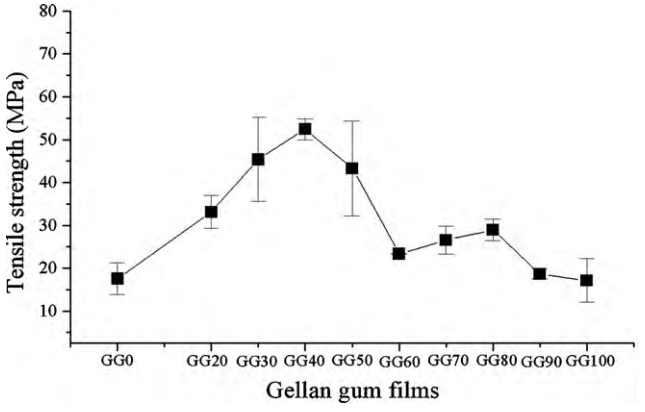

Fig. 2. The tensile strength of GG films cross-linked in various concentrations of ethanol with 15 mM EDC for 24 h.

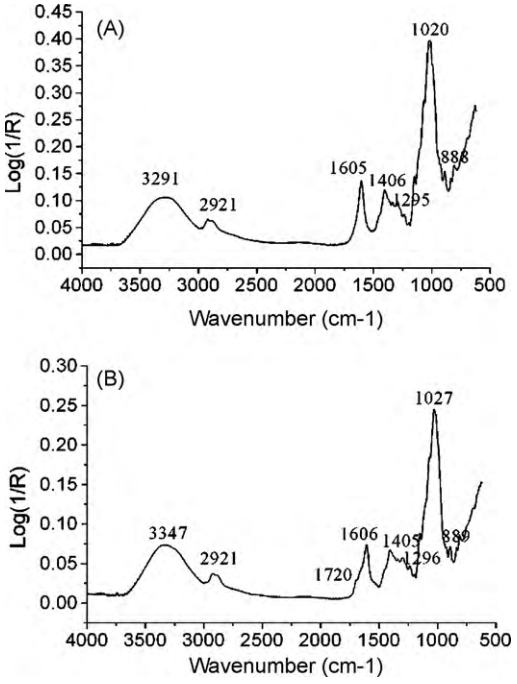

Fig. 3. FTIR spectra of non-cross-linked GG film (A) and cross-linked GG film (B).

3.3. FTIR characterization of GG film

Fig. 3A and B shows the FTIR spectrograms of non-cross-linked GG and GG40 films. Fig. 3A shows the assignment of the absorption band at 3291 cm^{-1} for stretching the –OH groups in GG. The band at 2921 cm^{-1} is due to the stretching vibrations of the $–CH_2$ group (Agnihotri, Jawalkar, & Aminabhavi, 2006; Xu, Li, Kennedy, Xie, & Huang, 2007), whereas those appearing at 1020 and 1149 cm^{-1} are due to ethereal and hydroxylic C–O stretching. The peaks at 1605 and 1405 cm^{-1} can be assigned to the characteristic absorption band of carboxyl in non-cross-link GG. The bending vibration of C–H appears at 888 cm^{-1} (Alupei, Popa, Bejenariu, Vasiliu, & Alupei, 2006; Sudhamani, Prasad, & Udaya Sankar, 2003). Fig. 3B shows both the FTIR spectrogram of GG40 film and a new absorption peak at 1720 cm^{-1} (Lee et al., 2005). This indicates that carboxyl grouped on β-D-glucuronic acid (Glcp A) of GG can generate an ester bond with -OH groups. It also causes the absorption peak of the -OH groups to shift to a higher wave number—3347 cm^{-1}, and the C–O stretching to shift from 1020 to 1027 cm^{-1}. However, the absorption peak of $–CH_2$ groups shows no shift both before and after cross-linking. These data indicate that the new absorption peak is not caused by residual EDC and confirms that the cross-linking reaction was successful.

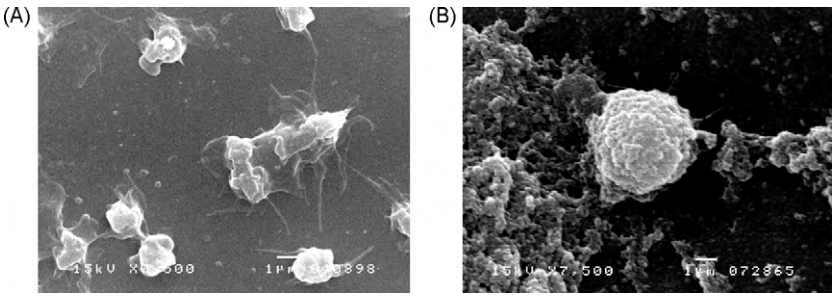

Fig. 4. The morphology of platelets absorbed on the surface of Glass (A) and GG40 (B) (SEM 7500×).

3.4. Platelet adhesion

Measurements performed using an Automatic Hematology Analyzer indicated that there was a large amount of platelet absorption in the positive control group ($6 \times 10^4/\mu L$). However, when the platelets encountered the GG40 film after 120 min, the amount of absorption on the film was lower than $1 \times 10^3/\mu L$ (the minimum limit measurable by the Analyzer). We used SEM to observe the surface of the GG40 film. The average number of absorbed platelets under each view (7500×) was found to be less than 1 (Fig. 4B). The SEM image was also used to observe the morphology of platelets absorbed on the base material due to their activation in the positive control group (glass). Obvious pseudo pods were observed on the platelets (Fig. 4A) (Mao et al., 2004). The platelets absorbed on the surface of the GG40 film were round in shape and without pseudo pods (Fig. 4B). The results confirm that GG40 film can resist the absorption of platelets and is a type of inert material for them.

3.5. Attachment and growth of L929 fibroblast cells on GG film

As an *in vitro* screening test for the adhesion capability of GG film to fibroblast, we inoculated the L929 fibroblast cells onto the GG40 film, cultured them for designated periods, and evaluated the cell viability with MTT assay. Fig. 5 shows the results of this MTT test. In the 24 h period following cell seeding, an absorbance unit of only 0.6 was displayed by the viable cells on the GG40 film as compared with the 1.1 units of cells grown on cultured flasks. This indicates that GG40 was able to inhibit cell adhesion attributable to the negatively charged surface (Lee et al., 2005). However, once the cells attached to the surfaces of the GG40 film or the flask, the attached cells proliferated at approximately equal rates, as indicated by the similarity in slope of increasing absorbance. This implies that GG40 film disfavored cell adhesion and exhibited a nontoxic effect on the attached cell.

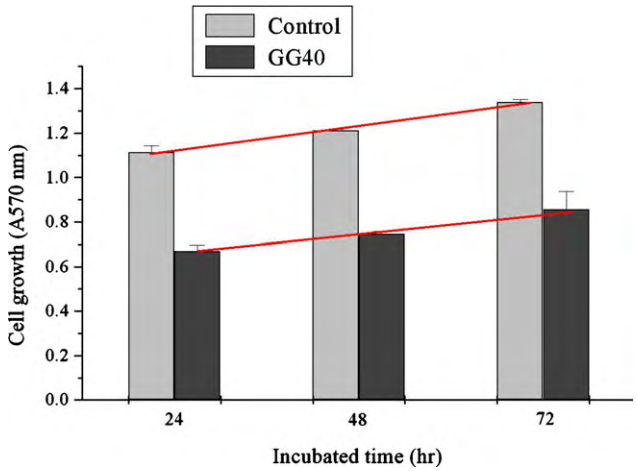

Fig. 5. Viability of L929 cells after 24, 48, and 72 h exposures to GG40 ($n = 5$, results are given as mean values, bars represent standard deviation).

3.6. In vivo biocompatibility

Researcher implanted HA film (positive control) and GG40 films in the SD-rats' subcutaneous tissue to evaluate inflammation reaction. In the positive control, histological examination showed that there were inflammatory cells in contact between the material and the tissue on the 3 days after implanting (Fig. 6A) (Fernández-Cossío, León-Mateos, Sampedro, & Oreja, 2007; Fulzele, Satturwar, & Dorle, 2007). On the 14 days after implanting, there were no residual materials in the gross examination. Examination of histology (Fig. 6B) found that there was no inflammation of cells, which indicates that HA film does not cause chronic inflammation. After we had implanted GG40 films for 3 days and 14 days, histological examination showed the presence of Neutrophil (N) and Macrophage (M) (Fig. 6C and D). Neutrophil is an indicator of acute inflammation, and Macrophage is an indicator of chronic inflammation (Wang et al., 2006; Kweon, Song, & Park, 2003). This proves that GG40 film may lead to both acute and chronic inflammation. Continuous follow-up studies of the inflammation caused by the GG40 film showed that the histological section (Fig. 6E) had only a few macrophages from the implanted materials existing after 1 month. In terms of visual observations, residual materials could be seen after the GG40 film had been implanted for 1 month. This suggests that long-term follow-ups are important. In addition to inflammation, histological section showed subcutaneous tissue with no fibrosis, stromal reaction, or vaccularity (Macleod, Williams, Sanders, & Green, 2005). Based on the results, it can be concluded that GG40 film demonstrate good *in vivo* biocompatibility.

3.7. In vivo wound healing

3.7.1. Gross examination

In this study, Duoderm and GG40 film were placed on the SD-rat wound sites 5, 15, and 24 days after surgery for observation in macro vision. After 5 days, the dressing and the wound in the control group showed severe adhesion, and hemorrhage occurred upon removal of the dressing (Fig. 7A). In the GG40 group, we observed a healthy, clean wound, pink and red in color, during the healing process. In addition, the GG40 film adhered to the wound only slightly, and we were able to remove it from the wound surface without causing further trauma (Fig. 7D). After 15 days, it was difficult to separate the Duoderm from the tissue, which resulted in considerable tissue bleeding during removal of the dressing. As a result, the wound healing process was prolonged. Nevertheless, for GG40 dressings, the wound was kept moist and no signs of inflammation

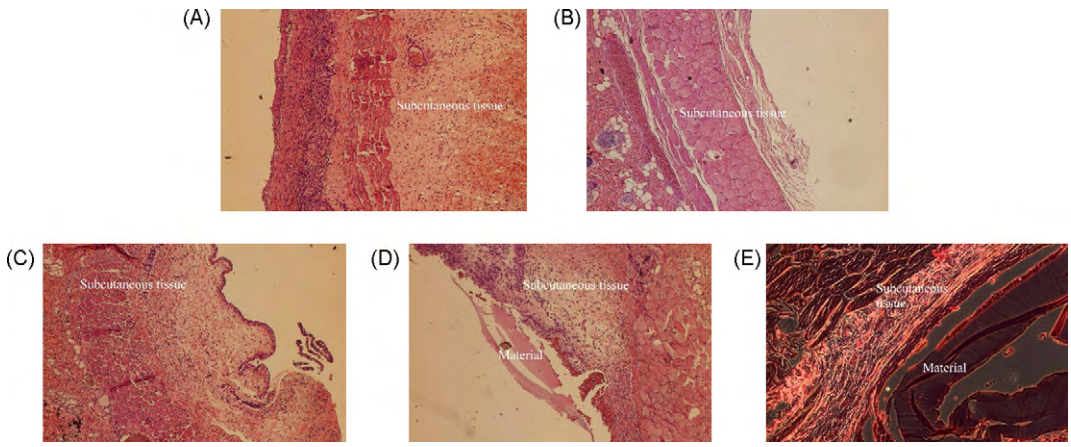

Fig. 6. Micrograph of rat subcutaneous tissue response to hyaluronic acid (HA, control) and GG40 film (HE stain 200×). (A) HA-3 days, (B) HA-14 days, (C) GG40-3 days, (D) GG40-14 days, and (E) GG40-30 days after surgery.

and infection were observed (Fig. 7B and E). In a previous study, Winter reported that the epithelialization process can be accelerated if the wound is kept moist (Winter, 1962; Winter & Scale, 1963). The epidermal cells migrate more easily over a moist wound surface than under a scab in dry wounds (Yang et al., 2010). After 24 days, for both Duoderm and GG40 dressings, most wound tissues repaired themselves with no obvious residual scar tissue.

This study calculated the reduction in the wound defect area by measuring the wound area size before and after fixed intervals of time (Balakrishnan, Mohanty, Umashankar, & Jayakrishnan, 2005). In the control group, 5, 15, and 24 days after surgery, the wound size reduction (%) was $31 \pm 7\%$, $45 \pm 9\%$, and $89 \pm 3\%$, respectively. In the experimental group, 5, 15, and 24 days after surgery, the wound size reduction (%) was $34 \pm 3\%$, $54 \pm 11\%$, and $88 \pm 3\%$, respectively. The wound size reduction in the control and experimental group at 15 days showed statistically significant differences ($P < 0.05$). On the 24 days after the operation, the difference in wound size reduction between the two groups was not statistically significant ($P > 0.05$). Based on the above results, it can be conclude that in the first few days after operation the effects of GG40 film in promoting healing are superior to those of Duoderm.

3.7.2. Histological examination

Rat skin tissue includes several different parts, such as the epidermis, dermis, musculoautaneous layer, and subcutaneous tissue. The histological sections showed a regenerated tissue structure and inflammation at the epidermis and dermis layers (Li et al., 2008; Ong, Wu, Moochhala, Tan, & Lu, 2008). In the control group, the epidermis had regenerated on the 5 days after surgery (Masson's trichroma stain, Fig. 8A). However, some tissues had separated because the structure was incomplete. The GG40-film-treated group (Fig. 8D) exhibited a deeply stained epidermis color similar to that of the original tissue, which indicates that the structure was more compact. In addition, inflammatory cells were visible in the regenerated dermis, the control group and the test group, which suggests that inflammation occurred. According to literature (Balakrishnan et al., 2005), inflammation is inevitable in the early stages of a wound because dressing is a foreign matter. Additionally, the regenerated dermis in the experimental group showed many fibrous extracellular ground substances. It is evident the regeneration of tissues occurred faster in the experimental group. Again, both groups displayed regenerated blood vessels, and no bacterial colonies were found in either group. On the 15 days after surgery,

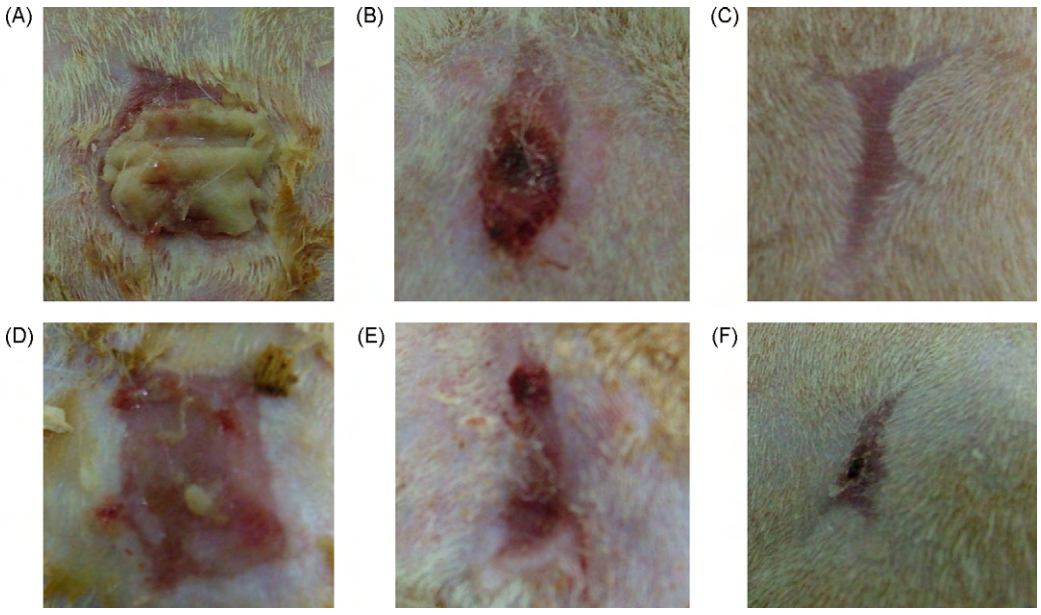

Fig. 7. Representative photographs of macroscopic appearance of a 2 cm × 2 cm wound excised on rat, control wounds at 5 (A), 15 (B) and 24 days (C), and GG40 film wounds at 5 (D), 15 (E) and 24 days (F) after surgery.

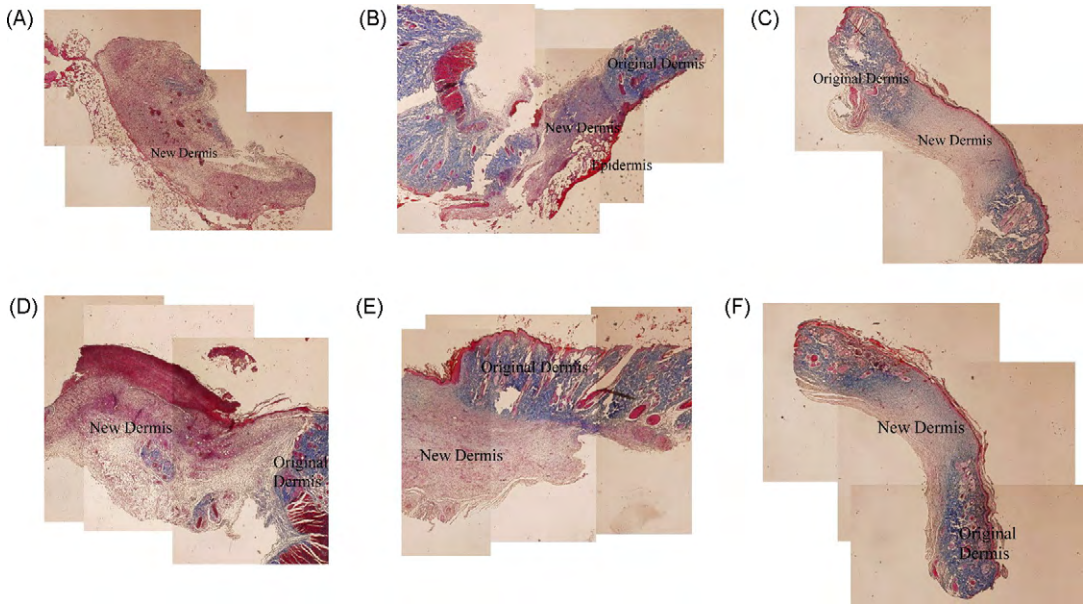

Fig. 8. Micrograph of wound re-epithelialization in control group 5 (A), 15 (B) and 24 days (C), and GG40 film group 5 (D), 15 (E) and 24 days (F) after surgery (Masson's trichrome stain 100×).

the generated epidermis in the control group (Fig. 8B) was still not compact, and the regenerated dermis showed round nucleus cells. In the test group (Fig. 8E), the cells in the dermis were primarily fibrous. Regardless of the group, integration occurred at the junction between regenerated and original tissues and exhibited a higher level of tissue healing. On the 24 days after surgery, the histological sections (Fig. 8C and F) showed that the amount of regenerated tissue was similar between the control and test group. This length of time is sufficient to allow the majority of wound tissues to repair and explains the similarities between the two groups.

The extracellular ground substances of the skin tissues primarily contain type 1 collagen. To determine the distribution of extracellular ground substances of the regenerated tissues, we utilized the Masson's trichrome stain to stain the collagen (Li et al., 2008). The basis for the relative quantity of collagen is the blue color value of the tissue sections (if blue is stronger, the value is lower). In the control group, 5, 15, and 24 days after surgery, the color value of blue was 110 ± 16, 91 ± 12, and 75 ± 7, respectively. In the experimental group, 5, 15, and 24 days after surgery, the color value of blue was 108 ± 22, 88 ± 6, and 70 ± 3, respectively. The data indicate that color value decreases with increase in time in both the control and experimental groups. This also indicates that the amount of collagen secreted increases with increase in time. Five and fifteen days after the surgery, the color values between the two groups showed no statistically significant difference ($P > 0.05$). Twenty-four days after the surgery, the color value of the test group was lower than that of the control group ($P < 0.05$), which suggests that the test group had larger amounts of collagen secretion. This result confirms that GG40 film is a better option than the commercially used Duoderm during the wound healing process. In addition, the results could also be used to estimate the differences between regenerated collagen and collagen of the original tissues. The collagen of the original tissues was blue (color value 108 ± 5), whereas the regenerated collagen was bluish grey. The collagen of the original tissues was loosely distributed whereas the regenerated collagen was more compact. Past studies have reported that inflammation reaction can delay the regeneration of tissues (Jones, Edwards, & Thomas, 2004). In this study, GG40 film showed a high level of biocompatibility and excellent physical properties, which could help promote wound healing.

4. Conclusion

GG is one of many microbial polysaccharides used in drug delivery, tissue engineering, and in the food industry, but not in surgical applications such as wound healing and dressing. Therefore, this study prepared water-insoluble GG films and studied their characterization and biological properties to expand future medical applications. EDC can activate the galacturonic acid residues contained within the GG molecule. To prevent EDC hydrolysis in water, we applied ethanol as the reaction solvent, with results suggesting that highest gel content was observed when the GG was cross-linked in 40% ethanol. From the FTIR analysis, the mechanism of EDC cross-linking in the GG was the condensation reaction between the carboxyl and hydroxyl group. Because polysaccharide films normally possess poor mechanical strength, the results obtained in this study indicate that GG40 film is suitable for potential applications in skin replacement. With respect to *in vitro* biocompatibility, MTT assay revealed that GG40 is compatible with both L929 fibroblast cells and blood. With respect to *in vivo* biocompatibility, subcutaneous implantation showed that GG40 caused slight inflammation in the first few days after operation, but no fibrosis or stromal reaction in either long-term or short-term implantation. In the wound healing test, GG40 film demonstrated good physical properties and biocompatibility, and proved to be capable of accelerating wound repair. In conclusion, EDC cross-linked GG film has great potential for future use in clinical applications.

References

Agnihotri, S. A., Jawalkar, S. S., & Aminabhavi, T. M. (2006). Controlled release of cephalexin through gellan gum beads: Effect of formulation parameters on entrapment efficiency, size, and drug release. *European Journal of Pharmaceutics and Biopharmaceutics*, *63*, 249–261.

Alupei, I. C., Popa, M., Bejenariu, A., Vasiliu, S., & Alupei, V. (2006). Composite membranes based on gellan and poly(*N*-vinylimidazole). Synthesis and characterization. *European Polymer Journal*, *42*, 908–916.

Balakrishnan, B., Mohanty, M., Umashankar, P. R., & Jayakrishnan, A. (2005). Evaluation of an in situ forming hydrogel wound dressing based on oxidized alginate and gelatin. *Biomaterials*, *26*, 6335–6342.

Bemiller, J. N. (1996). Structure-property relationships of water-soluble polysaccharides. *Journal of Applied Glycoscience*, *43*, 377–384.

Ezequiel, S. C.-J., Edel, F. B-S., Alexandra, A. P. M., Wander, L. V., & Herman, S. M. (2009). Preparation and characterization of chitosan/poly(vinyl alcohol) chemically crosslinked blends for biomedical applications. *Carbohydrate polymers*, *76*, 472–481.

Fernández-Cossío, S., León-Mateos, A., Sampedro, F. G., & Oreja, M. T. (2007). Biocompatibility of agarose gel as a dermal filler: Histologic evaluation of subcutaneous implants. *Plastic & Reconstructive Surgery*, *120*, 1161–1169.

Fialho, A. M., Moreira, L. M., Granja, A. T., Popescu, A. O., Hoffmann, K., & Sá-correia, I. (2008). Occurrence, production, and applications of gellan: Current state and perspectives. *Applied Microbiology and Biotechnology*, *79*, 889–900.

Fulzele, S. V., Satturwar, P. M., & Dorle, A. K. (2007). Novel biopolymers as implant matrix for the delivery of ciprofloxacin: Biocompatibility, degradation, and in vitro antibiotic release. *Journal of Pharmaceutical Sciences*, *96*, 132–144.

Ishihara, K., Nishiuchi, D., Watanabe, J., & Iwasaki, Y. (2004). Polyethylene/phospholipid polymer alloy as an alternative to poly(vinylchloride)-based materials. *Biomaterials*, *25*, 1115–1122.

Jansson, P. E., Lindberg, B., & Sandford, P. A. (1983). Structural studies of gellan gum, an extracellular polysaccharide elaborated by Pseudomonas elodea. *Carbohydrate Research*, *124*, 135–139.

Jay, A. J., Colquhoun, I. J., Ridout, M. J., Brownsey, G. J., Morris, V. J., Fialho, A. M., et al. (1998). Analysis of structure and function of gellans with different substitution patterns. *Carbohydrate Polymers*, *35*, 179–188.

Jones, S. G., Edwards, R., & Thomas, D. W. (2004). Inflammation and wound healing: the role of bacterials in the immune-regulation of wound healing. *The International Journal of Lower Extremity Wounds*, *3*, 201–208.

Kenji, I., & Ikada, Y. (1997). Preparation of cross-linked hyaluronic acid films of low water content. *Biomaterials*, *18*, 189–195.

Kuo, S. M., Chang, S. J., Niu, C. C., Lan, C. W., Chen, T. W., & Yang, C. Z. (2009). Guided tissue regeneration with use of β-TCP/chitosan composite membrane. *Journal of Applied Polymer Science: Applied Polymer Symposium*, *112*, 3127–3134.

Kwangwoo, N., Tsuyoshi, K., Seiichi, F., & Akio, K. (2010). Preparation of a collagen/polymer hybrid gel designed for tissue membranes. Part I: Controlling the polymer-collagen cross-linking process using an ethanol/water co-solvent. *Acta Biomaterialia*, *6*, 403–408.

Kweon, D. K., Song, S. B., & Park, Y. Y. (2003). Preparation of water-soluble chitosan/heparin complex and its application as wound healing accelerator. *Biomaterials*, *24*, 1595–1601.

Lee, M. W., Hung, C. L., Cheng, J. C., & Wang, Y. J. (2005). A new anti-adhesion film synthesized from polygalacturonic acid with 1-ethyl-3-(3-dimethylaminopropyl) carbodiimide crosslinker. *Biomaterials*, *28*, 3793–3799.

Leicht, P., Siim, E., Dreyer, M., & Larsen, T. K. (1991). Duoderm application on scalp donor sites in children. *Burns*, *17*, 230–232.

Li, H., Fu, X., Zhang, L., Huang, Q., Wu, Z., & Sun, T. (2008). Research of PDGF-BB gel on the wound healing of diabetic rats and its pharmacodynamics. *Journal of Surgical Research*, *145*, 41–48.

Macleod, T. M., Williams, G., Sanders, R., & Green, C. J. (2005). Histological evaluation of Permacol as a subcutaneous implant over a 20-week period in the rat model. *British Journal of Plastic Surgery*, *58*, 518–532.

Mao, C., Yuan, J., Mei, H., Zhu, A., Shen, J., & Lin, S. (2004). Introduction of photocrosslinkable chitosan to polyethylene film by radiation grafting and its blood compatibility. *Materials Science & Engineering C: Biomimetic Materials, Sensors and Systems*, *24*, 479–485.

Monotalbetti, C. A. G. N., & Falque, V. (2005). Amide bond formation and peptide coupling. *Tetrahedron*, *61*, 10827–10852.

Ong, S. Y., Wu, J., Moochhala, S. M., Tan, M. H., & Lu, J. (2008). Development of a chitosan-based wound dressing with improved hemostatic and antimicrobial properties. *Biomaterials*, *29*, 4323–4332.

Pollock, T. (1993). Gellan related polysaccharide and the genus Spingomonas. *Journal of General Microbiology*, *139*, 1939–1945.

Ramires, P. A., Miccoli, M. A., Panzarini, E., Dini, L., & Protopapa, C. (2005). In vitro and in vivo biocompatibility evaluation of a polyalkylimide hydrogel for soft tissue augmentation. *Journal of Biomedical Materials Research Part B: Applied Biomaterials*, *72*, 230–238.

Rinaudo, M. (2004). Role of substituents on the properties of some polysaccharides. *Biomacromolecules*, *5*, 1155–1165.

Sen, Majumder, P., & Bhowmick, A. K. (1999). Surface-and bulk-properties of EPDM rubber modified by electron beam irradiation. *Radiation Physics and Chemistry*, *53*, 63–78.

Sudhamani, S. R., Prasad, M. S., & Udaya Sankar, K. (2003). DSC and FTIR studies on gellan and polyvinyl alcohol (PVA) blend films. *Food Hydrocolloid*, *17*, 245–250.

Vijayabaskar, V., Tikku, V. K., Bhowmick, & Anil, K. (2006). Electron beam modification and crosslinking: Influence of nitrile and carboxyl contents and level of unsaturation on structure and properties of nitrile rubber. *Radiation Physics and Chemistry*, *75*, 779–792.

Wang, C. M., Gong, Y. H., Lin, Y. M., Shen, J. B., & Wang, D. A. (2008). A novel gellan gel-based microcarrier for anchorage-dependent cell delivery. *Acta Materialia*, *4*, 1226–1234.

Wang, T. W., Sun, J. S., Wu, H. C., Tsuang, Y. H., Wang, W. H., & Lin, F. H. (2006). The effect of gelatin–chondroitin sulfate–hyaluronic acid skin substitute on wound healing in SCID mice. *Biomaterials*, *27*, 5689–5697.

Winter, G. D. (1962). Formation of the scab and the rate of epithelialization of superficial wounds in the skin of the young domestic pig. *Nature*, *193*, 293–294.

Winter, G. D., & Scale, J. T. (1963). Effect of air drying and dressings on the surface of a wound. *Nature*, *197*, 91–92.

Xu, X., Li, B., Kennedy, J. F., Xie, B. J., & Huang, M. (2007). Characterization of konjac glucomannan–gellan gum blend films and their suitability for release of nisin incorporated therein. *Carbohydrate Polymers*, *70*, 192–197.

Yang, J. M., Yang, S. J., Lin, H. T., Wu, T. H., & Chen, H. J. (2008). Chitosan containing PU/poly(NIPAAm) thermosensitive membrane for wound dressing. *Materials Science & Engineering C: Biomimetic Materials, Sensors and Systems*, *28*, 150–156.

Yang, X., Yang, K., Wu, S., Chen, X., Yu, F., Li, J., et al. (2010). Cytotoxicity and wound healing properties of PVA/ws-chitosan/glycerol hydrogels made by irradiation followed by freeze-thawing. *Radiation Physics and Chemistry*, *79*, 606–611.